Copper Transparent Antennas on Flexible Glass by Subtractive and Semi-Additive Fabrication for Automotive Applications

Jack P. Lombardi III[*], Robert E. Malay [*], James H. Schaffner[†], Hyok Jae Song[†], Ming-Huang Huang[‡],
Scott C. Pollard[‡], Mark D. Poliks[*] and Timothy Talty[§]

[*]*Department of System Science and Industrial Engineering*
Binghamton University, Binghamton, New York 13902
Email: mpoliks@binghamton.edu
[†]*HRL Laboratories, LLC, Malibu, California*
[‡]*Corning Research and Development Corporation, Corning, New York*
[§]*General Motors, Warren, Michigan*

Abstract—**There has been an increasing need for antennas in automotive applications, for communications applications, such as cellular, satellite radio, and the burgeoning fields of self-driving/networked vehicles and 5G. These applications demand alternatives to traditional vehicle antennas, including transparent antennas able to be unobtrusively mounted to vehicle windows. Flexible glass provides a high quality transparent and flexible substrate for the fabrication of these antennas, and that is amenable to low cost roll-to-roll manufacturing. Sheet scale prototype transparent antennas were fabricated in copper using etch back and semi-additive processes, with conventional processes and facilities, and using materials and processes amenable to roll-to-roll fabrication. This shows that flexible glass could be used in existing lines and facilities with little modification, in addition to roll-to-roll processing. Fabricated antennas were tested on-vehicle and show good performance, with similar gain figures for baseline solid antennas, etched transparent antennas, and semi-additive transparent antennas.**

Keywords-**flexible electronics; mobile antennas; vehicular and wireless technologies**

I. Introduction

Antennas are a key part of the radios and communication systems used in daily life, and are an increasingly important component of automobiles. This is due to the increasing connectivity and sensing now being demanded of our vehicles. This includes navigation with GPS signals, communication and data via cellular networks, entertainment and information via satellite radio, and short range radar systems for collision avoidance [1], [2]. This is all in addition to the upcoming expansion in connectivity and communication brought about by 5G, which will greatly increase vehicle communications, both vehicle to overhead or terrestrial transceivers and vehicle to vehicle [3]–[5] While monopole and shark fin antennas have been dominant [1], this increasing need, along with aesthetics and cost, is driving other alternatives. One such alternative is that of a transparent flexible antenna. This antenna would be advantageous in that it could be unobtrusively mounted to the windows of a vehicle, matching the curve of the glass

and located where terrestrial and satellite signals can be received. This necessitates the use of a flexible, transparent substrate, and Corning® Willow® Glass fits this role, as well as having many other advantages. These include high transparency, excellent surface quality, high thermal and chemical stability, and a refractive index that matches other glasses [6]–[9]. Fabrication of this antenna would also need to be low cost and high volume to meet the needs of the automotive industry.

These two requirements drive the selection of roll-to-roll (R2R) manufacturing. R2R has been demonstrated in the document printing industry, and can be applied for the fabrication of antennas and structures for RFID, increasing throughput and lowering cost [10]–[12]. R2R manufacturing has advantages specific to glass, where it removes the handling of sheets of glass and allows for the easier handling via rolls [8], [13]. The Center for Advanced Microelectronic Manufacturing (CAMM) at Binghamton University specializes in the development of R2R manufacturing processes, especially processes involving Willow Glass [14], [15]. Due to the scale of these tools and quantities of materials needed, there are restrictions on processing, such as no strong acid etching or precious metal deposition, due to safety or cost. The work conducted here will be on individual substrates of 100μm thick glass, 100mm wafers in initial tests and 150mm x 150mm sheets for the antennas, but done with an eye towards R2R manufacturing and compatible with CAMM processing. The wafers and sheets fabricated here will use low cost etched or semi-additive copper, and weak acids compatible with CAMM tools to create conductive meshes, and then transparent antennas. Transparent antennas, both rigid and flexible, have been created using mesh conductors as transparent conductors. Escobar *et al.* and Elmobarak Elobaid *et al.* demonstrated transparent antennas using free standing wire mesh screens that were patterned and attached to a dielectric (Lexan polycarbonate or polydimethylsiloxane) to form patch antennas [16], [17]. Guan *et al.*, Hong *et al.*, and Lee and Jung also used mesh conductors for

the fabrication of single layer antennas, with Guan *et al.* utilizing printed meshes of silver paste with lines as small as 2.5μm [18], while Hong *et al.*, and Lee and Jung used copper meshes to create microstrip patch antennas as well as receivers for wireless power transfer, with lines approximately 20μm wide [19], [20].

This work shows that the initial prototyping on Willow Glass can be done with conventional lithographic tools and plating rigs, and allows processes to be developed in wafer and sheet scale before transitioning to R2R manufacturing. In that vein, this work will describe the initial experiments done with 100mm wafers of Willow Glass, where the initial grids of copper were produced, using both etching and semi-additive methods. Following the results of these tests, antennas are then fabricated on 150mm x 150mm sheets, building on the results of the 100mm wafers. These antennas are then characterized, and shown to be highly transparent, as well as having good RF properties in on-vehicle tests.

II. Test Pattern and Antenna Design

A. Transparent Conductor Design

The transparent antennas fabricated here are based on the idea that transparent conductors can be made by simply cutting holes into a layer of a conductor, making it a mesh, with a certain ratio between the width of the conductor lines (w) and the period of lines (p), as shown in Fig. 1a. The sheet resistance and transparency of the layer will then vary based on this ratio and mesh material can be approximated with effective properties. A study of this trade off was conducted using the electromagnetic analysis software program FEKO® [21], and the results are shown in Fig. 1b, c. These studies indicate that for a layer of Cu 2-2.5μm thick, a period to width ratio of 10-15 is needed to meet goals of 80% transmission with a sheet resistance of 0.3$\Omega/\square$ or less at microwave frequencies. With these theoretical results, a design consisting of 25.4mm x 25.4mm blocks of these grids was created, with width-period variants

(in micrometers) of 5-50, 5-75, 5-100, 10-100, 10-150, 10-200, and 30-450. This allows the different variations to be created in one fabrication, and the transmission and sheet resistance to be measured using a four point probe, with the area assumptions for four point probe measurements satisfied [22]. This design is slightly modified based on the fabrication process used, with the field inverted, so only the plated areas are opened, and additional openings added around edge of the wafer for the semi-additive process, to allow for electrical connection to the seed layer. An example of this design is shown in Fig. 2.
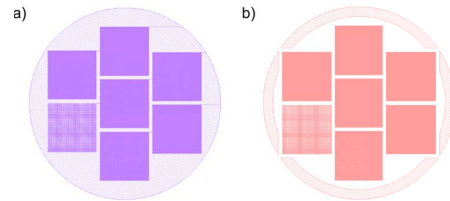

Figure 2. Screen captures of 100mm wafer designs with 25.4mm squares of meshed Cu for testing, with a) showing the subtractive and b) the semi-additive designs. Note that the tone of the designs are different, reflecting the different fabrication methods, and that the semi-additive design has windows on the edge of the wafer for electrical contact to the seed layer.

B. Antenna Design

The antenna used in this study was based on an automobile window glass mounted multiband antenna for cellular AMPS/PCS reception [23]. The antenna was scaled in size for operation in 4G LTE radio bands down to 690MHz and up to 2200MHz. A drawing of this design is shown in Fig. 3. While the focus of the design and fabrication are on the transparent antenna, solid designs are also fabricated to serve as baselines for performance comparisons.

To create the grid of conductors, a process was developed using AutoCAD and KLayout [24]. Both software packages have advantages, which are used to create a meshed version of the original design, while keeping smooth edges
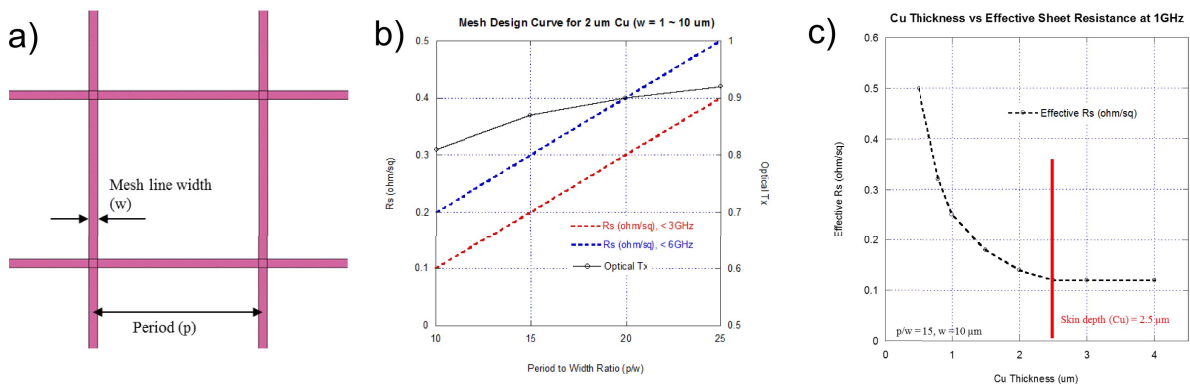

Figure 1. a) Diagram of mesh layout showing line width and period b) Design trade offs for sheet resistance at microwave frequencies and transparency, c) Design trade off between Cu thickness and effective sheet resistance
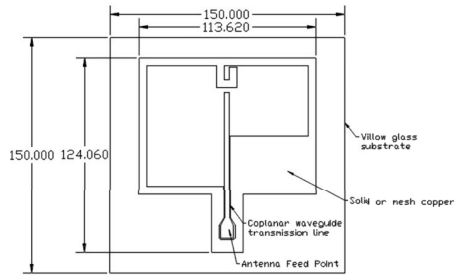
Figure 3. AutoCAD screen capture of antenna design on 150mm x 150mm flexible glass substrate. All dimensions are in millimeters

and producing an output that can be used for lithography. The meshing process started with the original antenna in AutoCAD in .DXF format, and an offset of the edges of the antenna is made. This is to create a smooth edge around the antenna, and create a boundary for the meshed area. The design is then imported to KLayout, and meshing done via a Boolean operation between an array of squares, representing the holes in the mesh, and the solid of the antenna, resulting in only the desired mesh being left. A subsequent Boolean operation is done to merge the edge created in AutoCAD with the meshed pattern, and a final Boolean may be done to reverse the field of the design for the etched process. Images of this process can be seen in Fig. 4. After the design was finalized, it was exported to the .GDSII file format. This format is used by the laser lithography system, and provided an unambiguous check of the design to be written.

III. FABRICATION

The fabrication of these antennas proceeded in two stages. The first was the fabrication of the 100mm wafers consisting of the 25.4mm squares of the Cu mesh. These were done

to validate the fabrication process and reduce risk, especially for the semi-additive process. Once these wafers were fabricated and characterized, fabrication of the antennas proceeded.

The fabrication process for these flexible samples was surprisingly conventional, and existing processes developed for conventional rigid substrates could be used with little to no modification. These included spin coating of resist, as well as the electroplating process. The biggest changes were in the handling of wafers and sheets. Sharp edges and point loads, like those produced by metal wafer tweezers, will readily break the glass by introducing defects that quickly propagate, so handling must be done with tools that have smooth, wide contacts to avoid this. To help with handling in certain steps, such as the wet etching, polyimide tape tabs are put on the sample to provide way to use tweezers without breakage. An example of these on the back of the 150mm x 150mm sheets is shown in Fig. 5. Due to the limitations

Figure 5. Photograph of 150mm x150mm sheets with tape tabs attached to the backside to aid in handling during etching.

of the tools used, manual removal of photoresist was used to complete the antennas. This consisted of removing the excess resist outside of the laser lithography write area, the ring around the antenna in the etched fabrications, and
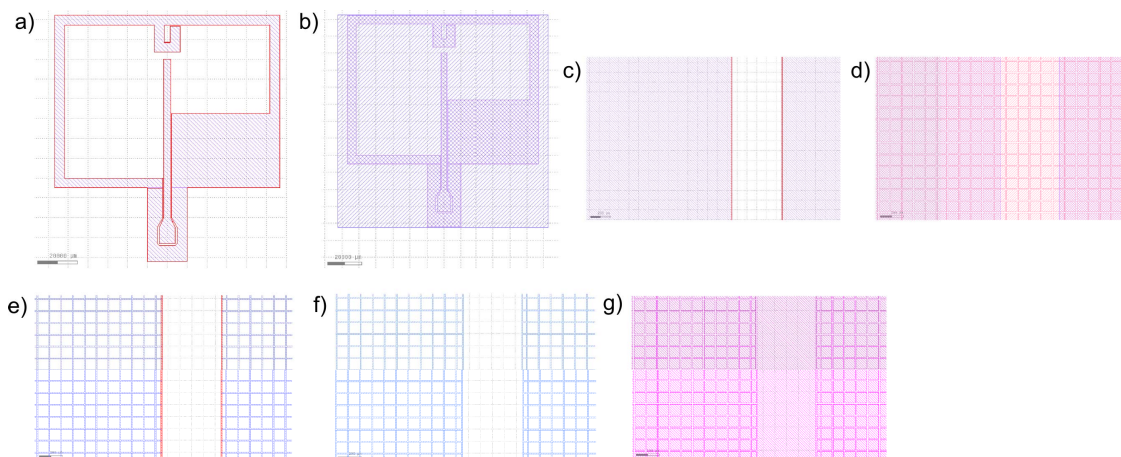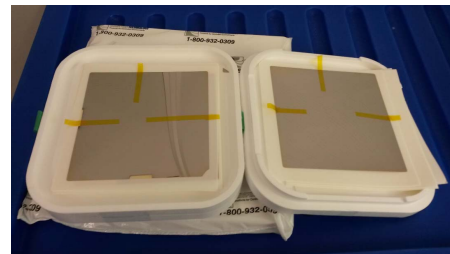

Figure 4. Screen captures from KLayout for the meshing of the antenna design. a) Solid antenna design on 125mm x 125mm write area b) Imported antenna design with 10μm offset edge (red), imported from Autocad c) Detail of offset edge d) Solid antenna design with blocks (pink) superimposed for mesh creation e) Mesh created from Boolean operation with blocks, shown with offset edge f) Merged mesh design and offset edge g) Boolean operation with 125mm x 125mm write area to create mesh design for writing in positive resist.

creating windows for contact with the seed layer in the semi-additive process. While further exposures could have been used to expose these areas, it was much faster and easier to manually remove the resist with solvent. It should be noted that the use of R2R can eliminate the need for these tricks, and that all the process steps demonstrated here can be ported to the R2R facilities at CAMM. A flow chart of these fabrications is shown in Fig. 6.
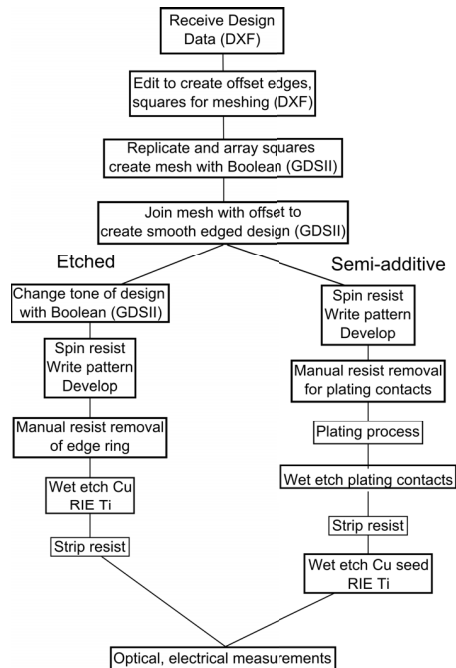

Figure 6. Flow chart of antenna fabrication process, for both etched and semi-additive antennas.

A. Etch Process

The samples fabricated by etching were able to be processed as one would expect any etch-back fabrication. First, metals are deposited on the as-received Willow Glass using a KDF in-line sputtering system. A 100nm Ti adhesion layer was followed by a nominally 1μm Cu layer. The 1μm Cu layer was chosen as the 2μm Cu was found too difficult to process. The next step was photolithography, where Microposit S1813 photoresist was spin coated nominally 1μm thick. It was found that both wafers and the larger squares could be adequately coated using the same spin parameters and dispensing more resist for the larger sheets. The spin coated sheets were not as uniform as the coated wafers, but were still usable. The resist was exposed using a Heidelburg Instruments μPG 101 laser direct write lithography system. This allowed for direct imaging of the designs, and easy design modifications, since no masks needed to be made. For the antenna fabrication, three writes were used; one for the antenna design, and two that were offset to the top and

bottom of the design, to allow for easier removal of excess photoresist "ring". These three writes are shown in Fig. 7.

The exposed sample was then developed, and the excess photoresist manually removed from antenna samples. The Cu layer was then etched using ammonium persulfate (APS) mixed from anhydrous crystals at a concentration of 20g/200mL at room temperature. This etchant was chosen due to restrictions on the chemistries available at CAMM, and based on our previous work [14]. While the 100mm wafers could be supported for etching in a wafer holder, the 150mm sheets were handled by the previously mentioned tape tabs. The etch took approximately 2 minutes to clear all Cu. The Ti adhesion layer was then etched using a Nano Master NRP-4000 PECVD/RIE system. A standard SiO_2 etch recipe was used to etch the Ti clear, with a process time of 5 minutes. A final solvent cleaning was done to remove any resist on the sample.

B. Semi-additive Process

The semi-additive process also started with the KDF in-line sputtering system, but with depositions of a 100nm Ti adhesion layer followed by a 100nm Cu seed layer. Photolithography to create a plating mask was then accomplished by spin coating MicroChem SPR 220 photoresist to a nominal thickness of 4μm. Again, the same spin parameters could be used for the wafers and sheets, increasing the amount of resist to help ensure a uniform coating. The design was then exposed using the Heidelburg Instruments μPG 101 laser direct write lithography system, and the resist developed. The wafers were able to be fully exposed, with windows to the seed layer opened in the write, but the antenna sheets required a manual resist removal step to create these windows. The next step was to copper plate. This was done with rigs that were compatible with existing
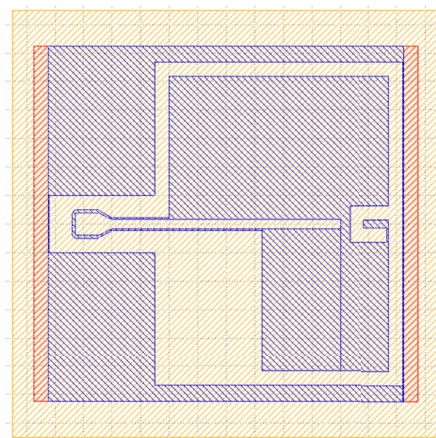

Figure 7. Example of using multiple designs with offsets to expose a larger area in an etch design, showing the first write (blue), additional write areas (red), and substrate area (orange). The orange substrate ring around the written areas was the area for manual resist removal.

fixtures and the bath chemistry. Rigs were created for the 100mm wafers and 150mm x 150mm sheets of glass, and used 316 stainless steel and FR-4. Mechanical restraint and electrical connection to the seed layer was made by stainless steel clips. These clips were polished to ensure there were no burs or sharp edges in contact with the glass. Using care and even pressure, these clips could be tightened to hold the glass samples without breakage, and these rigs are shown in Fig. 8. The plating process consisted of a 30 second immersion in a sulfuric acid solution, followed by the plating in a copper sulfate bath. The plating times varied based on the type of sample, with 3 minutes for a 100mm wafer, 4:30 minutes for a mesh antenna and 5:30 minutes for a solid antenna. These different times were a result of the different amounts of material to be plated and different plating rig used. Following the plating of the antenna sheets, the thick Cu where the clips made contact would need to be etched. To do this, each edge of the sheet was immersed in Transene CE-200 ferric chloride based etchant to etch off the thick Cu at these areas. This step was not done on the wafers, as the presence of these pads didn't affect the characterization of the test blocks. The resist was then stripped, and the Cu seed layer etched with the same APS etchant as stated above, with an etch time of approximately 4.5 minutes. The same RIE etch as described above was then used to remove the Ti adhesion layer. After these etches, the sample was complete, with Cu traces 2-2.5μm thick.

IV. RESULTS

A. Optical and Electrical Results

The incremental development of making wafers before antennas created preliminary results and a screening experiment for which mesh pattern should be used for the actual antenna fabrication. Characterization of these fabricated grids consisted of electrical and optical characterization, using a Jandel Model RM3000 four point probe to determine sheet resistance and a Filmetrics F20-UV reflectometer configured for transmission for optical transparency, calibrated

using a bare Willow Glass wafer. Photographs of the etched sample are shown in Fig. 9 and semi-additive in Fig. 10. Plots of optical transmission are shown in Fig. 11
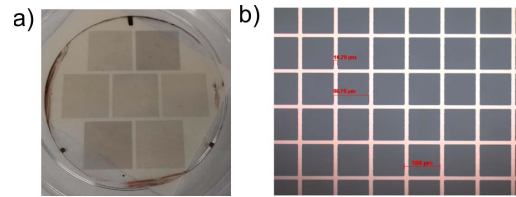
Figure 9. Images of a 100mm test wafer for etched meshes, with a) photograph of the wafer and b) micrograph of 10-100 mesh.
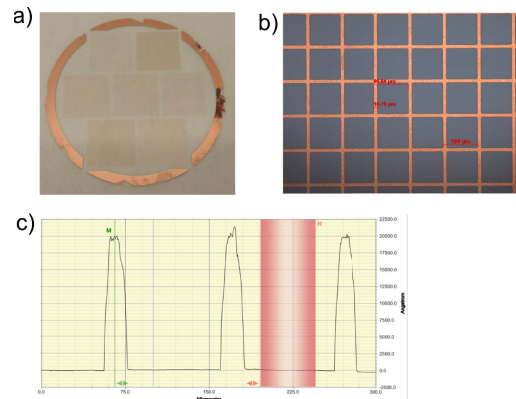
Figure 10. Images of 100mm test wafer for semi-additive meshes, with a) photograph of the wafer and b) micrograph of 10-100 mesh and c) stylus profilometer sweep verifying semi-additive mesh thickness at 2μm, shown as 20000Å.

and Fig. 12, while changes in sheet resistance and optical transmission as a function of the mesh type and fabrication are shown in Fig. 13. Based on these results, it was decided to use the 10-100 line-period combination, as this provided a good result for both fabrication processes, with transmission near 80% and sheet resistance no larger than 0.2$\Omega/\square$.

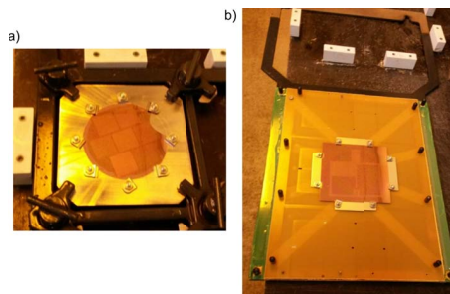Antennas were then fabricated with that mesh using both

Figure 8. Photographs of plating rigs, with a) rig for 100mm wafers, designed to fit into rack used for plating flex PCBs and b), rig used for plating 150mm x 150mm sheet, designed to fit into rack used for PCB plating. Note the stainless steel bars visible through the FR-4 backing that provide electrical connection.
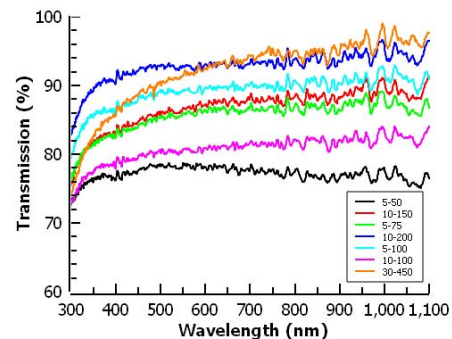

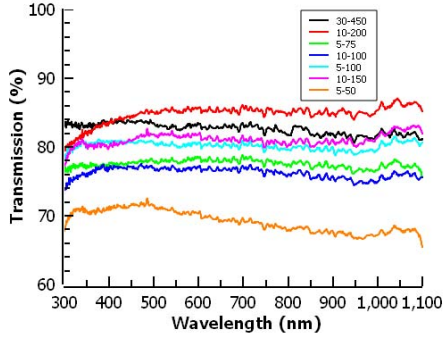Figure 11. Transmission spectra for 25.4mm blocks of mesh made by etching.

Figure 12. Transmission spectra for 25.4mm blocks made by semi-additive processing.
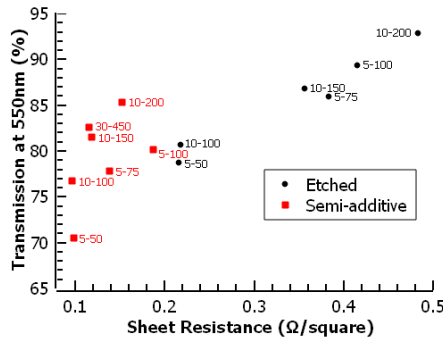

Figure 13. Scatter plot of sheet resistance and transmission for mesh samples fabricated by etching and semi-additive processes.

fabrication methods. While many antennas were fabricated, only a few were later RF tested. Those tested antennas are shown in Fig. 14, with their characteristics listed in Table I. These characteristics are measured in the large square of the antenna, and in line with the results of the wafers.

B. On-Vehicle Testing

As mentioned previously, a sample of antennas was selected for on-vehicle RF testing. This testing took place at
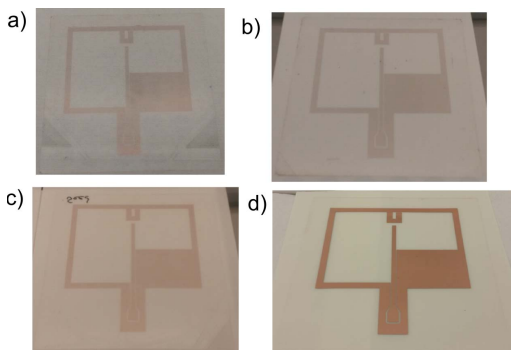

Figure 14. Photographs of antennas that were RF tested, with a) EM 4 b) EM 5 c) PM 1 d) ES 3.

Table I
CHARACTERISTICS OF TESTED ANTENNAS

Name	Transmission at 550nm (%)	Sheet Resistance (Ω/□)	Thickness (μm)
Etched Mesh 4 (EM 4)	85	0.489	0.75
Etched Mesh 5 (EM 5)	80	0.441	0.75
Plated Mesh 1 (PM 1)	80	0.081	2.5
Etched Solid 3 (ES 3)	N/A	0.02	1

Oakland University. This antenna range provided a roll-on roll-off capability for measuring vehicle antennas, where a vehicle was spun on a turntable while a goniometer mounted antenna measured the emitted field, as shown in Fig. 15. Prior to the measurements, the fabricated antennas were slot die coated with an adhesive that allowed the antennas to be attached and removed from automotive window glass, and coaxial pigtails with SMA connectors attached with conductive epoxy to provide electrical connection. At Oakland University, measurements were made with antennas mounted on the windshield of a sport utility vehicle as shown in Fig. 16. Two orientations on the windshield of a vehicle were used, as shown in Fig. 17, and measurements made for a variety of LTE frequencies in the range of 1700-2200 and 700-900MHz, for both vertical (V) and horizontal (H) polarizations.

While many measurements were made, difficulties in data collection allowed for only one complete data set for the comparison of fabrication methods. This set consists of only measurements made for all the antennas in the vertical orientation. A key metric for automotive antenna measurements is the linear average gain. This average is taken over a 360° azimuth sweep at 5° elevation increments, with 0° perpendicular to the ground. The linear average gain gives an indication of the antenna efficiency at each elevation angle. The linear average gain as a function of angle for each

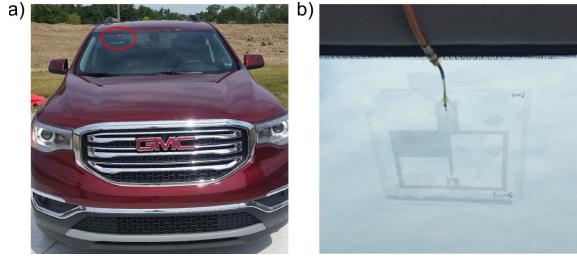Figure 15. Photograph of vehicle antenna range at Oakland University.

Figure 16.   Antenna mounting for on-vehicle RF testing, with a) front view of vehicle with antenna circled in red b) photograph of PM 1 antenna from inside of vehicle.
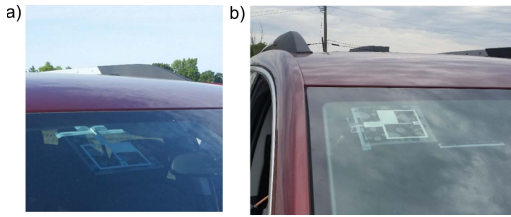

Figure 17.   Photographs of EM 3 antenna showing the a) vertical and b) horizontal orientations used for testing.
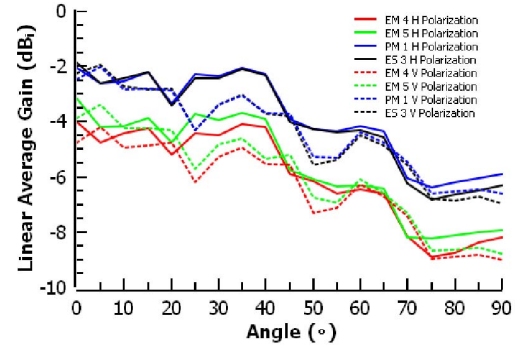

Figure 18.   Plot of linear average gains in the high band (1700-2200MHz) for on-vehicle antenna tests.

Figure 19.   Plot of linear average gains in the low band (700-900MHz) for on-vehicle antenna tests.

antenna and polarization are shown in Figs. 18 and 19, for the measured high and low frequency ranges, respectively. For these plots the average gain is converted to dB_i after the averages are calculated; for these curves dB_i is the ratio of the power measured for the elevation angle to the total power that would be radiated isotropically.

Looking at these linear average gains, it can be seen that there is little difference between the etched mesh antennas for either band or polarization, with high band measurements closely overlapping and low band measurements showing a difference of less than $2dB_i$. The semi-additive mesh antenna data is nearly identical to the solid reference antenna, and both show approximately 2-3dB_i higher gain as compared to the etched meshes in both bands and polarizations. This observation of very similar performance is also shown in 3D plots of the measured gain, as shown in Fig. 20. The high performance of the semi-additive mesh antenna can be partly attributed to the thicker mesh conductor, which mitigates RF loss due to the skin depth. Overall, all these antennas did have gains good enough for use in a wireless communication system, although they were approximately 2dB less than the conventional roof mounted LTE antennas. While increased losses may be present, these antennas would be implemented as part of a multiple input multiple output (MIMO) system, where the performance of below roof line LTE antennas like these have demonstrated LTE data throughput as good or better than the LTE throughput of roof mounted antennas [25].

V. Conclusion

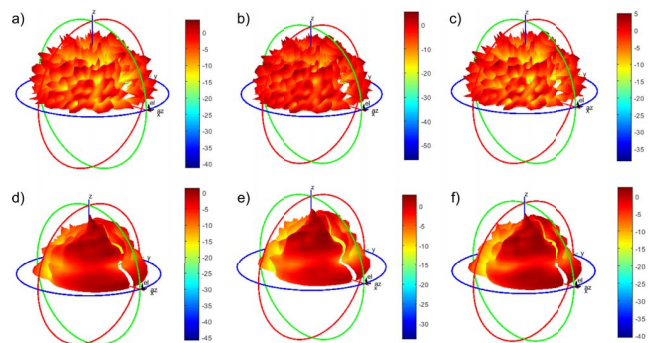Flexible transparent antennas on Corning Willow Glass have been demonstrated and tested on a vehicle. These

Figure 20.   3D visualizations of the observed antenna gain (dB_i) for the H polarization at a high band frequency of 2110MHz and low band frequency of 717 MHz, with a) EM 5 high band, b) PM 1 high band, c) ES 3 high band, d) EM 5 low band, e) PM 1 low band, and f) ES 3 low band. Note that the visualizations are orientated such that the front of the vehicle is pointing to the lower right.

antennas were fabricated using a copper mesh, created with subtractive and semi-additive processes. These processes were demonstrated in a sheet format, but with materials and processes compatible with roll-to-roll manufacturing. This manufacturing method allows for low cost antennas, ideal for automotive use, via high throughput production with low cost copper conductors. The antennas themselves perform well, with transparency greater than 70% while having sheet resistance as low as $0.2\Omega/\square$. On-vehicle RF testing confirms that these antennas perform well, with solid and semi-additive transparent mesh antennas having nearly identical performance, while the thinner etched mesh antenna had a marginal decrease in performance. This demonstrates the feasibility and utility of these transparent antennas for automotive communications. Further development can improve performance of these antennas, and allow for the implementation and maturation of roll-to-roll electronics fabrication.

ACKNOWLEDGMENT

REFERENCES

[1] B. D. Pell, E. Sulic, W. S. Rowe, K. Ghorbani, and S. John, "Advancements in automotive antennas," in *New Trends and Developments in Automotive System Engineering*. InTech, 2011.

[2] K. Solbach and R. Schneider, "Review of Antenna technology for millimeter wave automotive sensors," in *Microwave Conference, 1999. 29th European*, vol. 1. IEEE, 1999, pp. 139–142.

[3] "Experience the Future of Mobility 5g Automotive Association." [Online]. Available: http://5gaa.org/5g-technology/experience-the-future/

[4] "Paving the way towards 5g 5g Automotive Association." [Online]. Available: http://5gaa.org/5g-technology/paving-the-way/

[5] "A look ahead at 5gs impact on the automotive industry," May 2017.

[6] S. M. Garner, S. C. Lewis, and D. Q. Chowdhury, "Flexible glass and its application for electronic devices," in *2017 24th International Workshop on Active-Matrix Flatpanel Displays and Devices (AM-FPD)*, Jul. 2017, pp. 28–33.

[7] M. Junghhnel and S. Garner, "Glass meets flexibility," *Vakuum in Forschung und Praxis*, vol. 26, no. 5, pp. 35–39, Oct. 2014.

[8] S. M. Garner, K. W. Wu, Y. C. Liao, J. W. Shiu, Y. S. Tsai, K. T. Chen, Y. C. Lai, C. C. Lai, Y. Z. Lee, J. C. Lin, X. Li, and P. Cimo, "Cholesteric Liquid Crystal Display With Flexible Glass Substrates," *Journal of Display Technology*, vol. 9, no. 8, pp. 644–650, Aug. 2013.

[9] M. Junghhnel, S. Weller, and T. Gebel, "P-65: Advanced Processing of ITO and IZO Thin Films on Flexible Glass," *SID Symposium Digest of Technical Papers*, vol. 46, no. 1, pp. 1378–1381, Jun. 2015.

[10] Accrington, "On a roll," *The Economist*, Jul. 2016.

[11] N. Savage, "Roll to Roll Electronics Manufacturing Rolls On," *IEEE Spectrum: Technology, Engineering, and Science News*, Jan. 2016.

[12] R. R. Sndergaard, M. Hsel, and F. C. Krebs, "Roll-to-Roll fabrication of large area functional organic materials," *Journal of Polymer Science Part B: Polymer Physics*, vol. 51, no. 1, pp. 16–34, Jan. 2013.

[13] H. Tamagaki, Y. Ikari, and N. Ohba, "Roll-to-roll sputter deposition on flexible glass substrates," *Surface and Coatings Technology*, vol. 241, pp. 138–141, Feb. 2014.

[14] R. Malay, A. Nandur, J. Hewlett, R. Vaddi, B. E. White, M. D. Poliks, S. M. Garner, M.-H. Huang, and S. C. Pollard, "Active and passive integration on flexible glass substrates: Subtractive single micron metal interposers and high performance IGZO thin film transistors," in *Electronic Components and Technology Conference (ECTC), 2015 IEEE 65th*. IEEE, 2015, pp. 691–699.

[15] M. D. Poliks, Y. L. Sung, J. Lombardi, R. Malay, J. Dederick, C. R. Westgate, M. H. Huang, S. Garner, S. Pollard, and C. Daly, "Transparent Antennas for Wireless Systems Based on Patterned Indium Tin Oxide and Flexible Glass," in *2017 IEEE 67th Electronic Components and Technology Conference (ECTC)*, May 2017, pp. 1443–1448.

[16] E. R. Escobar, N. J. Kirsch, G. Kontopidis, and B. Turner, "5.5 GHz optically transparent mesh wire microstrip patch antenna," *Electronics Letters*, vol. 51, no. 16, pp. 1220–1222, 2015.

[17] H. A. Elmobarak Elobaid, S. K. Abdul Rahim, M. Himdi, X. Castel, and M. Abedian Kasgari, "A Transparent and Flexible Polymer-Fabric Tissue UWB Antenna for Future Wireless Networks," *IEEE Antennas and Wireless Propagation Letters*, vol. 16, pp. 1333–1336, 2017.

[18] N. Guan, H. Tayama, S. Kaushal, and Y. Yamaguchi, "A wire-grid type transparent film UWB antenna," in *2017 IEEE-APS Topical Conference on Antennas and Propagation in Wireless Communications (APWC)*, Sep. 2017, pp. 166–169.

[19] S. Hong, Y. Kim, and C. Won Jung, "Transparent Microstrip Patch Antennas With Multilayer and Metal-Mesh Films," *IEEE Antennas and Wireless Propagation Letters*, vol. 16, pp. 772–775, 2017.

[20] H. H. Lee and C. W. Jung, "Magnetic resonantwireless power transfer for transparent laptop applications using -metal mesh film," *Microwave and Optical Technology Letters*, vol. 59, no. 11, pp. 2781–2785, Nov. 2017.

[21] "FEKO - EM Simulation Software." [Online]. Available: https://www.feko.info/

[22] F. M. Smits, "Measurement of Sheet Resistivities with the Four-Point Probe," *Bell System Technical Journal*, vol. 37, no. 3, pp. 711–718, May 1958.

[23] H. J. Song, C. R. White, J. H. Schaffner, A. Berkaryan, and E. Yasan, "Multi-function antenna," U.S. Patent US 8,704,719 B2, Nov., 2010.

[24] "KLayout Layout Viewer And Editor." [Online]. Available: http://www.klayout.de/index.php

[25] J. H. Schaffner, H. J. Song, A. Bekaryan, T. Talty, D. Carper, and E. Yasan, "Scanner based drive test LTE capacity measurements with MIMO antennas placed inside the vehicle," in *2015 IEEE International Conference on Microwaves, Communications, Antennas and Electronic Systems (COMCAS)*, Nov. 2015, pp. 1–4.